

Effective Potential and Topological Photon Spheres: A Novel Approach to Black Hole Parameter Classification

Jafar Sadeghi ^{*1}, Mohammad Ali S. Afshar ^{*2}

^{*}Department of Physics, Faculty of Basic Sciences,
University of Mazandaran P. O. Box 47416-95447, Babolsar, Iran

Abstract

In this article, we anchor our analysis on the premise that the presence of a photon sphere is an intrinsic characteristic of any ultra-compact gravitational structure with spherical symmetry. Utilizing the concept of a topological photon sphere, we categorize the behaviors of diverse gravitational models based on the structure of their photon spheres. This innovative approach enables us to define boundaries for black hole parameters, which subsequently allows us to classify the model as either a black hole or a naked singularity. Indeed, we will demonstrate that the existence of this reciprocal relationship between the gravitational structure and the presence of a photon sphere offers a unique advantage that can be directly and inversely harnessed. Furthermore, we present a precise correlation between the behavior of the defined effective potential and the total topological charge for each model. Through an independent examination of the effective potential, we show that a gravitational model typically exhibits naked singularity behavior when at least one effective potential minimum (a stable photon sphere) protrudes beyond the event horizon. Finally, we will compare the effect of adding perfect fluid dark matter to the models under study and observe the impact of this quantity on the behavior of the photon sphere and the extent of their dominance.

Keywords: Black hole, Photon sphere, Topological classification, Different parameters.

Contents

1	Introduction	2
2	The topological path to the photon sphere	4
3	Explanation of topological charges based on properties of effective potential	8

¹Email: pouriya@ipm.ir

²Email: m.a.s.afshar@gmail.com

4	Effective potential and topological photon sphere as a tool for classification	13
4.1	Photon Sphere and perfect fluid dark matter black hole(PFDM)	14
4.2	Photon Sphere and charged AdS black hole with perfect fluid dark matter(CPFDM)	17
4.3	Photon Sphere and Euler-Heisenberg black hole	20
4.4	Photon Sphere and Euler-Heisenberg black hole surrounded by PFDM	23
4.5	Photon Sphere and Black Holes With Nonlinear Electrodynamics(NLE)	27
5	Conclusions	31

1 Introduction

In the study of ultra-compact gravitational objects, the simplest and initial step for distinguishing between black hole configurations and naked singularities is the examination of the metric function followed by the identification of the event horizon. The emergence of a metric function is, in fact, the result of a complex amalgamation of initial conditions such as energy conditions and geometric compatibility with the equations of general relativity, among others, which ultimately manifest themselves in the form of a mathematical-physical metric function for the models. The remaining weaknesses of the resulting models, are then covered by conjectures such as the Weak Cosmic Censorship Conjecture (WCCC) through the creation of an event horizon. This conjecture posits that singularities that appear while solving Einstein's equations must be concealed behind an event horizon. This is because if singularities were observable from the rest of space-time, causality would be jeopardized, and physics would lose its predictive power. It seems that this condition, rather than being a powerful scientific statement, is an attempt to cover the current scientific and instrumental weaknesses and our lack of understanding of the geometric spacetime that we are, in fact, unable to describe.

It should be noted that the non-fulfillment of the WCCC condition does not imply 'non-existence' or 'absence' but rather the 'existence' of a space-time which, although it has its own gravitational effects, our current information is not enough to decipher this space, and even today, extensive studies are being conducted on the possibility and conditions of the emergence and observation of these regions. For example, space-time singularities created during gravitational collapse can be observed by an external observer, and the visibility of a spacetime singularity depends on the initial conditions of the collapsing matter [1–14]. Therefore, knowing under what conditions our model behaves like a black hole and from what range it transitions to an ultra-compact object without an event horizon (naked singularity) is important. But the regions of the naked singularity may also be involved in the results under certain conditions. Hence, the extent of their influence must also be defined.

After constructing the initial metric function based on effective theories in action, what will most influence the location of the event horizon are the values considered for the parameters

related to each theory. In simple terms, these parameters' permissible range can be studied based on the roots of the metric function. However, it is clear that this method will definitely not be applicable in determining the dominance range of the naked singularity.

So, in order to gain a better understanding of the overall space surrounding an ultra-compact object, one must seek a potential function that provides a more comprehensive answer to how the gravity of this structure affects the entire surrounding space. In pursuit of such a function, we know on one hand that the nature of attractive structures, whether in their classical or quantum form, necessitates the existence of stable and unstable circulating loops. On the other hand, in gravity, the presence of such loops around a black hole or an ultra-compact object has been well calculated both experimentally and observationally, as well as theoretically for different black hole models. In the observational study, investigators documented the presence of a distinct dark shadow, which emerged due to the gravitational deflection of light by the colossal black hole located at the nucleus of the massive elliptical galaxy M87. This phenomenon conclusively substantiates the existence of photon rings encircling the central dense object. [15–20] or, theoretically, Cunha et al. showed during their studies that, in spherical symmetry, standard black holes, as well as other ultra-compact objects (that can be with or without event horizon) in general relativity, can have planar circular photon orbits. In such a way that the stable type causes instability, and its unstable type could determine the shadows of the black hole [21]. Also, in a new paper it was shown in a geometrical proof that 'any spherically symmetric space-time that is asymptotically flat and has a horizon must contain a photon sphere, a spherical photon shell' [22]. Therefore, considering the above characteristics, it seems that the idea of the photon sphere can be used for a more precise classification of the space surrounding the ultra-compact structures.

To calculate the photon sphere in the usual way, one must go to the action and, after calculating the Lagrangian and Hamiltonian, extract the effective potential and then study the photon ring. But, in this work, instead of using the traditional method above for calculating the photon ring, which especially with the complication of the action requires more complex mathematical calculations, we propose the use of topological photon sphere. Of course, it must be stated that the use of topological photon spheres, in addition to fulfilling our need for spatial classification, will also bring other valuable benefits for us, which will be referred to at the appropriate time. As, we have stated, the foundation of our work in this article is predicated on the necessity of the photon sphere for ultra-compact object structures. However, to approach the topological photon sphere, we commence our study of the photon sphere from the point where Cardoso and his colleagues have articulated: "The mere observation of an unstable light ring is strong evidence for the existence of black holes", or, "The existence of a stable light ring is thus an unavoidable feature of any ultra-compact star" [23]. Then Cunha et al. showed during their studies that, in spherical symmetry, standard black holes, as well as other ultra-compact objects (that can be with or without event horizon) in general relativity, can have planar circular photon orbits. In such a way that the stable type causes instability, and its unstable type could

determine the shadows of the black hole [22]. Finally, after Cunha et al. which extended their work to spherically symmetric 4D black holes [26], ” Shao-Wen Wei” used this idea and” Duan” mapping, and extended the discussion of the photon ring to photon sphere with a topological approach. He stated that there exists at least one standard photon sphere outside the black hole not only in asymptotically flat space-time, but also in asymptotically AdS and dS space-time [24].

In this article, we will use the ”Wei” method to classify space based on the topological photon sphere behavior for different black holes. It means that, the topological current is non-zero only at the zero point of the vector field, which determines the location of the photon sphere. Therefore, one topological charge can be considered for each photon sphere. In the full exterior region, based on a specific range of parameters where the Total Topological Charge(TTC) is always equal to -1, the structure will be considered a black hole, and conversely. Moreover, on the same basis, for a naked singularity that has a vanishing topological charge, the TTC will be 0 [24] or +1 [25]. Ultimately, if neither of the above states occurs and, on the other hand, the metric function and effective potential within the studied range are without roots, due to the violation of the condition for the existence of a photon sphere in these regions, these areas will likely represent forbidden zones.

All above information give us motivation to arrange the paper as follows. In section 2, we briefly review the mathematical and physical foundations of the work. The Duan’s topological mapping and the effective potential are introduced, and then we state the circular null geodesic conditions. And finally, we combine the obtained relations and deduce the used calculation. In Section 3, we first address the advantages and disadvantages of utilizing this method and proceed to study the effective potential with greater precision in terms of physical concepts and the alignment of its graphical results with the TTC outcomes. We will endeavor to articulate the physical significance of the effective potential graph. In section 4,we will study and analyze different introduced models using this method and Finally, we have conclusions which are summarized in section 5.

2 The topological path to the photon sphere

Solving the metric function (1) based on the specific parameters only leads to an interval in which the radius of event horizon will remain real according to the desired parameters,

$$ds^2 = -dt^2 f(r) + \frac{dr^2}{g(r)} + (d\theta^2 + d\varphi^2 \sin(\theta)^2) h(r). \quad (1)$$

The event horizon, a null one-sided hypersurface that acts as a causal boundary, ensuring that the WCCC holds. But there are other areas where system behavior is still important to us (for example, naked singularities,the hypothetical gravitational singularity without an event horizon). The meaning of the above statements will be that, there are regions where the behavior of

the system is singular, and the metric function cannot help us to identify that region. For this reason, we must turn to concepts that, with greater precision and over a broader area, display the gravitational behavior of the model under study. Consequently, we explore the photon ring and photon sphere. The photon sphere is a null ring that is the lower bound for any stable orbit, showing the extreme bending of light rays in a very strong gravity. It has two types: unstable, where small perturbations make the photons either escape or fall into the black hole, and stable, where the opposite happens. The unstable type is useful for determining the black hole shadows, while the stable type causes spacetime instability [27].

Several methods can be used to study the photon sphere that among the different possible methods, in this work we considered the "Wei" topological method [24]. If we want to analyze the foundations of the work of this will be combination of basic concepts such as Poincaré section [28], Duan's topological current mapping theory and the necessary conditions for the existence of null geodesics.

In 1984, Yishi Duane conducted a pivotal analysis of the intrinsic structure of conserved topological currents within the SU(2) gauge theory. During this examination, Duane introduced the concept of topological flow associated with point-like systems akin to particles. This foundational work laid the groundwork for subsequent discussions on various forms of topological currents. [29]. In the first step, we consider a general vector field as ϕ which can be decomposed into two components, ϕ^r and ϕ^θ ,

$$\phi = (\phi^r, \phi^\theta), \quad (2)$$

also here, we can rewrite the vector as $\phi = \|\phi\|e^{i\Theta}$, where $\|\phi\| = \sqrt{\phi^a\phi^a}$, or $\phi = \phi^r + i\phi^\theta$. Based on this, the normalized vector is defined as,

$$n^a = \frac{\phi^a}{\|\phi\|}, \quad (3)$$

where $a = 1, 2$ and $(\phi^1 = \phi^r)$, $(\phi^2 = \phi^\theta)$. Now we introduce our antisymmetric superpotential as follows [24, 29],

$$\Upsilon^{\mu\nu} = \frac{1}{2\pi}\epsilon^{\mu\nu\rho}\epsilon_{ab}n^a\partial_\rho n^b, \quad \mu, \nu, \rho = 0, 1, 2,$$

and the topological current will be as,

$$j^\mu = \partial_\nu \Upsilon^{\mu\nu} = \frac{1}{2\pi}\epsilon^{\mu\nu\rho}\epsilon_{ab}\partial_\nu n^a\partial_\rho n^b.$$

Based on this, Noether's current and charges at the given Ω will be,

$$\partial_\nu j^\nu = 0$$

and

$$Q = \int_\Omega j^0 d^2x, \quad (4)$$

where j^0 is the charge density. By replacing ϕ instead of n and using the Jacobi tensor, we will arrive at,

$$j^\mu = \frac{J^\mu(X) \ln(||\phi||) \Delta_{\phi^a}}{2\pi}, \quad (5)$$

where $X = \frac{\phi}{x}$. By using two-dimensional Laplacian Green function in $\phi - mapping$ space, we have,

$$\ln(||\phi||) \Delta_{\phi^a} = 2\delta(\phi) \pi, \quad (6)$$

and the topological current will be,

$$j^\mu = J^\mu(X) \delta^2(\phi). \quad (7)$$

From the properties of δ , it is clear that j^μ is non-zero only at the zero points of ϕ^a , and this is exactly what we need to continue the discussion. Finally, by using the above relations and inserting them in relation (3), the topological charge become,

$$Q = \int_{\Omega} J^0(X) \delta^2(\phi) d^2x, \quad (8)$$

once again and this time around the topological charge Q , according to the characteristic of the δ function, it can be said that the charge is non-zero only at the zero point of ϕ . This results lead us how to use and calculate the photon sphere in the near future. Now, we are going to investigate the photon sphere and some null geodesics with static and spherical symmetry background (1), Here, we consider four-momentum and Hamiltonian condition for null geodesics,

$$\Pi = \frac{p^\nu p^\mu g_{\mu,\nu}}{2} = 0, \quad (9)$$

and the radial component of the null geodesic equations will be as [24],

$$\dot{r}^2 + V_{eff} = 0, \quad (10)$$

and

$$V_{eff} = g(r) \left(\frac{L^2}{h(r)} - \frac{E^2}{f(r)} \right), \quad (11)$$

where E and L represent the photon's energy and the total angular momentum, respectively. A circular null geodesic occurs at an extremum of the effective potential $V_{eff}(r)$, which is given by,

$$V_{eff} = 0, \quad \partial_r V_{eff} = 0. \quad (12)$$

These local extrema of the effective potential are equivalent to unstable and stable circular null geodesics, will correspond to a photon sphere and an anti-photon sphere. By Considering the equations(12) at the same time, we have following expression,

$$\left(\frac{f(r)}{h(r)}\right)'_{r=r_{ps}} = 0, \quad (13)$$

where prime is the derivative with respect to r . By rewriting(13), we will have,

$$f(r)h(r)' - f(r)'h(r) = 0. \quad (14)$$

The first term at the horizon will be disappear, but this case the second term usually remains non-zero, it means that r_{ps} and r_h do not coincide. According to the results and concepts of the above discussion, we are now in a place where we can start investigating the topological characteristics of the photon sphere.

So,here we Start this work by introducing a regular potential [6],

$$H(r, \theta) = \sqrt{\frac{-g_{tt}}{g_{\varphi\varphi}}} = \frac{1}{\sin \theta} \left(\frac{f(r)}{h(r)}\right)^{1/2}, \quad (15)$$

the discussion of potential will allow us to search for the radius of our photon sphere at,

$$\partial_r H = 0,$$

so, we can use a vector field $\phi = (\phi^r, \phi^\theta)$,

$$\begin{aligned} \phi^r &= \frac{\partial_r H}{\sqrt{g_{rr}}} = \sqrt{g(r)} \partial_r H, \\ \phi^\theta &= \frac{\partial_\theta H}{\sqrt{g_{\theta\theta}}} = \frac{\partial_\theta H}{\sqrt{h(r)}}. \end{aligned} \quad (16)$$

With the above definition ϕ , and recalling the relationships of the Duan's section, we now define the current and charge (3) for this new potential.

Furthermore, in light of relation (7) and the distinctive properties of the Dirac delta function, it can be inferred that the charges will manifest as non-zero exclusively at the loci where ϕ vanishes. Precisely at these junctures, the photon sphere is situated, thereby enabling the assignment of a topological charge Q to each photon sphere. Pursuant to equation (7), upon considering Ω as a manifold encompassing a singular zero point, subsequent analysis reveals that the charge Q is precisely commensurate with the winding number. Let C_i denote a closed, smooth, and positively oriented curve that encapsulates solely the i_{th} zero point of ϕ , while all

other zero points lie external to it.” So the winding number can be calculated by the following formula,

$$\omega_i = \frac{1}{2\pi} \oint_{C_i} d\Lambda, \quad (17)$$

where Λ is

$$\Lambda = \frac{\phi^2}{\phi^1}, \quad (18)$$

then the total charge will be,

$$Q = \sum_i \omega_i. \quad (19)$$

In conclusion, when the closed curve encompasses a zero point, the topological charge Q is precisely equivalent to the winding number. In instances where the curve encloses multiple zero points, Q will be the aggregate of the winding numbers corresponding to each zero point. Conversely, should the curve circumscribe no zero points, the resultant charge must invariably be zero.

3 Explanation of topological charges based on properties of effective potential

In his paper, 'Wei' demonstrated through the examination of winding numbers and the calculation of total charges for a model that whenever the TTC is -1, the structure will exhibit black hole behavior, and conversely, if the TTC is 0, the structure will be in the form of a naked singularity [24]. We have extended this work to show that in addition to the value of 0, the TTC value of +1 can also appear as a naked singularity [25]. However, in this section, we do not wish to delve into the meaning of the values mentioned above with regard to the field configuration around zero points and the analysis of winding numbers accordingly. Instead, we want to examine and study the concept of each of the values 0,+1, and -1 from the perspective of the effective potential equation (15). The potential defined in equation (15) for the study of the topological photon sphere, being a potential structure in its entirety, allows us to expect that classical principles governing potential functions can be utilized for its interpretation. This means that the extremum points on the potential curve play a significant role in justifying the physical behavior of the system dominated by the potential. If the potential curve has a local or global maximum, the system will leave this maximum upon the slightest perturbation. Conversely, if the system has a local minimum, it will tend to maintain its state unless there is a stronger global minimum in its vicinity, in which case, upon reaching the necessary disturbance, the system will move towards the global minimum for greater stability. Here, we will

demonstrate that this same behavioral pattern holds true for our topological potential as well.

Case I: TTC = -1

Typically, in such a scenario, one or several zero points emerge outside the event horizon in a manner that maintains the total charges at -1 and the structure with the unstable photon sphere remained in the form of a black hole.

To understand why, from an energy perspective, $TTC = -1$ corresponds to an unstable photon sphere, we have depicted a scenario for the Hayward black hole in Fig (1). As observed in Fig (1a), this black hole possesses a single zero point outside its event horizon, resulting in a TTC of -1, in accordance with reference [24]. In Fig (1b), we have plotted the potential $H(r)$. It is evident that this potential has a global maximum, which upon closer inspection of Fig (1c), is precisely located at the zero point or in other words, at the same location as the photon sphere. Given that this point represents a global maximum, any photon trapped within this potential will abandon this peak, or more precisely, the generating factor of this maximal potential (our black hole), at the slightest disturbance in pursuit of a state with lower energy. This signifies that we possess an unstable photon sphere, precisely the phenomenon of observational interest.

Case II: TTC = 0 or +1

From the energy perspective, these two states occur when one or several local or global minima appear outside the event horizon in such a way that they fully influence the nearby maxima. For a better understanding of the above concept, we examine these conditions for the Hayward model at a TTC of 0 and the Hyperscaling violation model [25] at a TTC of +1.

In a simplified assumption, devoid of complexities, if we consider the attraction in the form of potential function minima, as evident in Fig (2), it appears that in the Hayward model, an increase in the magnetic charge (g) aligns with gravity to enhance the gravitational strength of the model by creating local minima outside the event horizon. As we observe in Fig (2b), the presence of a minimum - a stable photon sphere - at $r = 1.389900878$ in the vicinity of a maximum - an unstable photon sphere - implies that even if a photon could leave the maximum under some perturbation, it would most likely be trapped in the nearest minimum, which would be our stable photon sphere. Two points must be noted here. First, this typically occurs when, from the metric function perspective, we are in a rootless region or what is known as a naked singularity space. In other words, the emergence of potential minima beyond the event horizon, which according to our assumption somehow confirms the extension of the model's intense gravity domain, becomes synonymous with a naked singularity. The second point to consider is how far increasing the parameters of the black hole (here g) will expand the dominance of stable photon spheres? In other words, does the naked singularity have its limits? In response, it should be said that, for example, in the Hayward model, the increase in the magnetic parameter is limited by the initial parameter values such as mass and de Sitter

radius, and for our choices ($m = 1, l = 1$), the parameter (g) will only be responsive up to the value of (1.21834146), and beyond this range, neither the metric function nor the potential function will practically have a response for space, which we refer to as the unauthorized region.

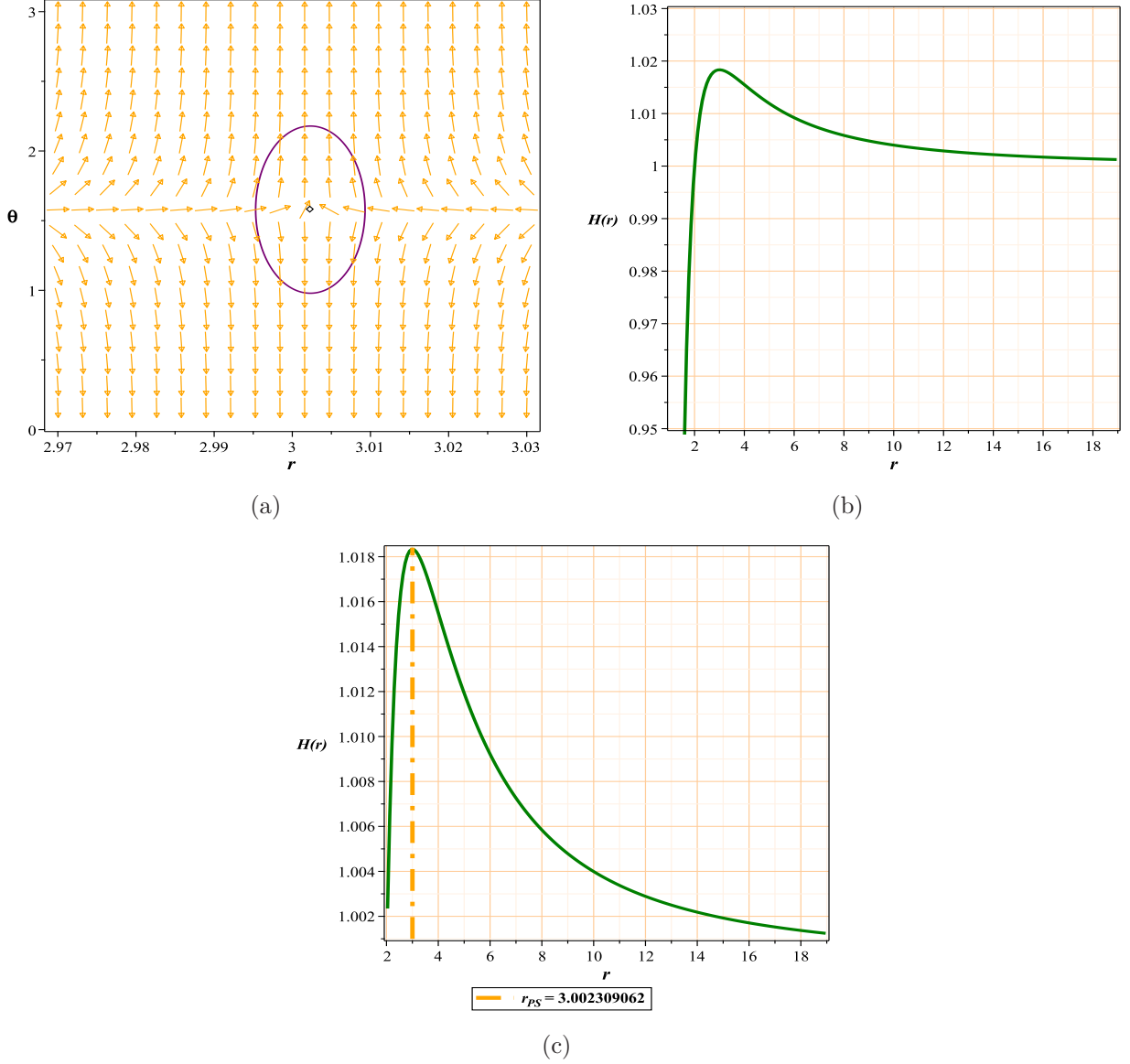


Figure 1: Fig (1a):The normal vector field n in the $(r - \theta)$ plane. The photon sphere is located at $(r, \theta) = (3.002309062, 1.57)$ with respect to $(g = -0.21834, m = 1, l = 1)$, (1b): the topological potential $H(r)$ for regular Hayward AdS black hole model, (1c): Enlarged details of diagram (1b)

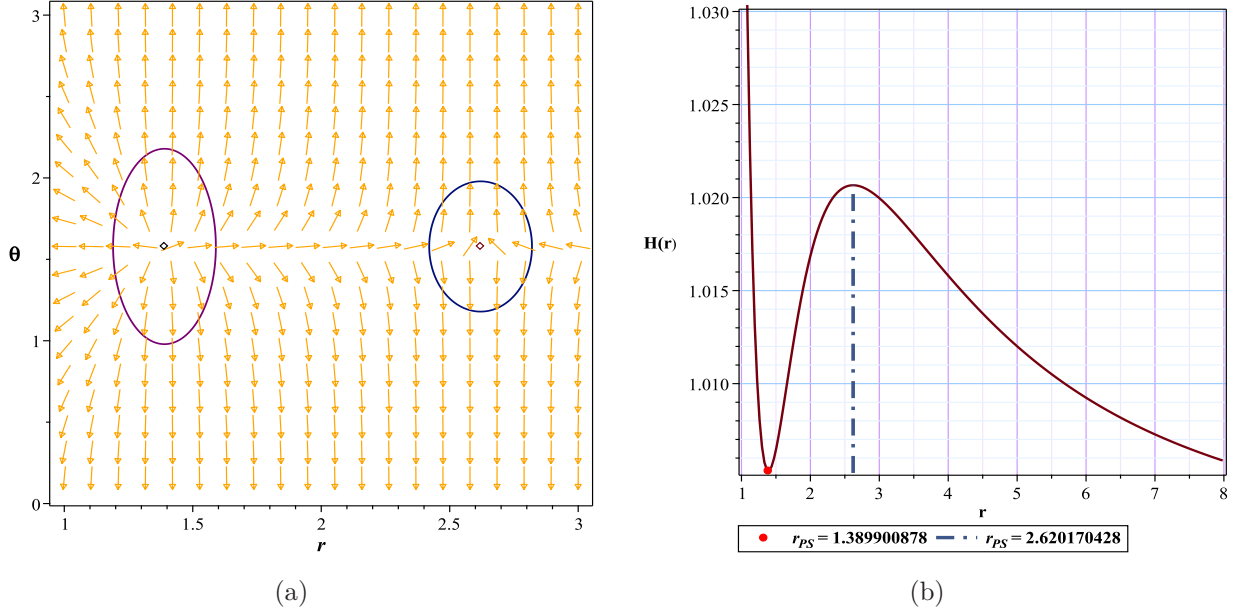


Figure 2: Fig (2a):The normal vector field n in the $(r - \theta)$ plane. The photon spheres are located at $(r, \theta) = (1.389900878, 1.57)$ and $(r, \theta) = (2.620170428, 1.57)$ with respect to $(g = 1.08, m = 1, l = 1)$, (2b): the topological potential $H(r)$ for regular Hayward AdS black hole model

In Fig(3), we encounter a scenario with a total topological charge (TTC) of +1. The fundamental difference between this state and the state with $TTC = 0$ is that here, due to the intensity of gravity, either no maximum is formed at all, or if an unstable photon sphere does form, as in Fig (3c) at $(r = 1.879279979)$, the sheer number of local minima in the vicinity is so great that the possibility of escape, even for photons, becomes unfeasible. Considering that if photons cannot escape such an environment, it can be inferred that no other massive particles would be able to escape either, effectively evoking conditions akin to those within an event horizon. Therefore, the emergence of a minimum in the effective potential outside the event horizon can be interpreted as a loss of all spatial information, and consequently, a violation of the Weak Cosmic Censorship Conjecture (WCCC), which equates to the manifestation of a naked singularity. However, we emphasize that the loss of information and spatial geometry does not imply non-existence, as the structure continues to exhibit gravitational evidence, namely the photon sphere, indicating its ongoing presence and vitality.

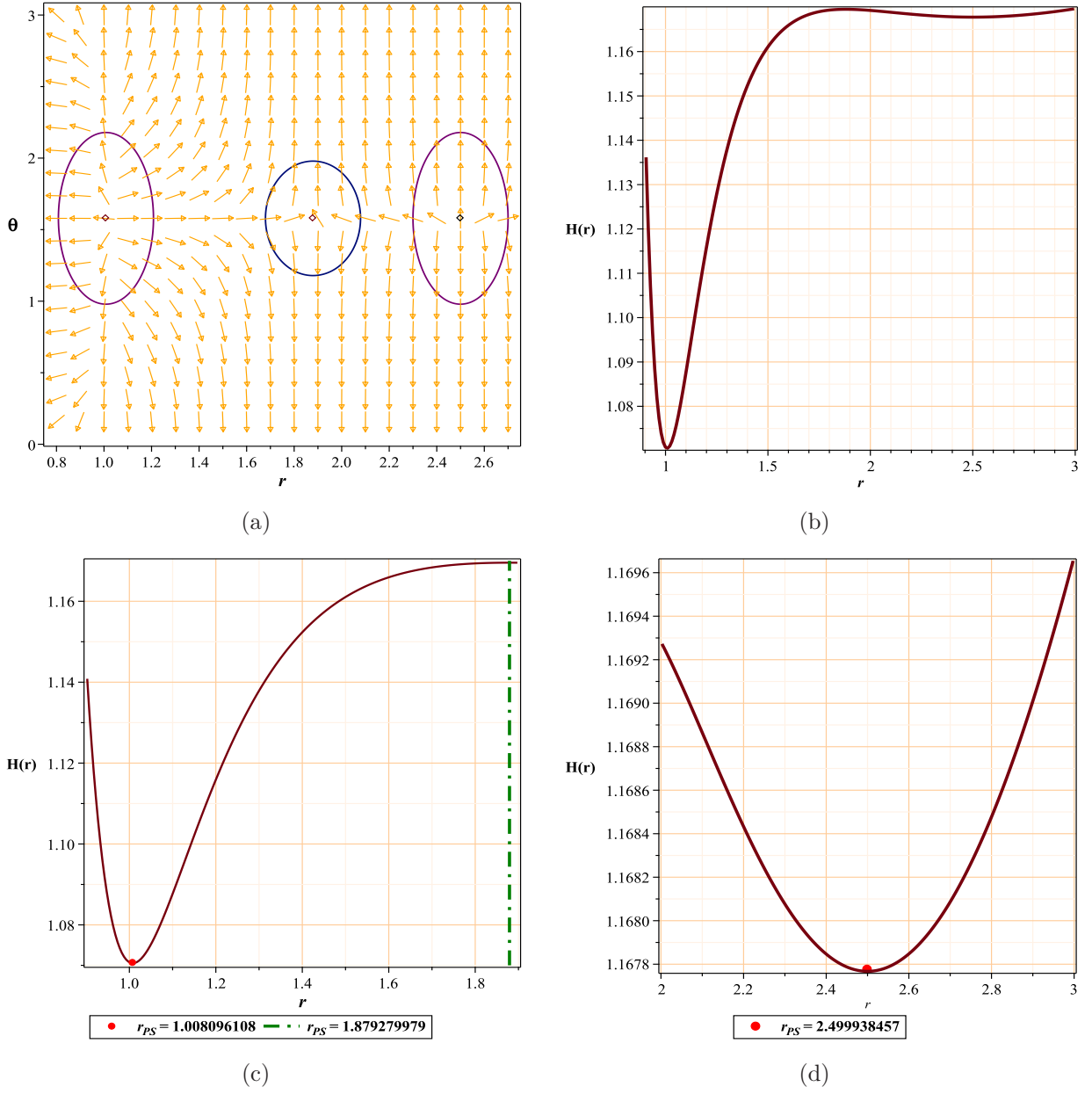


Figure 3: Fig (3a):The PSs are located at $(r - \theta) = (2.499938457, 1.57), (r - \theta) = (1.879279979, 1.57), (r - \theta) = (1.008096108, 1.57)$ with respect to $(q = 0.9, z = 1.1, M = 1.6, \theta = 0)$, (3b): the topological potential $H(r)$ for Hyperscaling violating model, (3c),(3d): Enlarged details of diagram (3b)

4 Effective potential and topological photon sphere as a tool for classification

Initially, it is prudent to briefly address the methodology of this study, along with its advantages and disadvantages, before proceeding to the selected models. In this work, we begin by constructing a potential function (15) utilizing the metric function of the model, which necessarily must be spherically symmetric. Based on this, we will construct the vector field ϕ (16). Subsequently, on the equatorial plane ($\theta = \frac{\pi}{2}$), we locate the roots of this vector field, which, as previously mentioned, will be the sites of the photon spheres. We then study the topological charge of these locations.

For the first time, based on the TTC and aligning its results with those of the effective potential graph, as well as the initial parameter values of the model and the roots of the metric function, we classify the space surrounding an ultra-compact object. We will also determine, with relatively good precision, the range of variation for the specific parameter of the model. It must be acknowledged that the utilization of this method carries its own set of advantages and disadvantages. The traditional approach to studying photon spheres necessitates the derivation of the Lagrangian from the action, followed by the construction of the Hamiltonian. Once the Hamiltonian is obtained, one must determine the effective potential and then proceed to study the photon sphere, taking into account the symmetries of the Killing vectors and their commutativity with respect to the model's symmetries. It is evident that the addition of various theories to the action can significantly complicate this pathway, both mathematically and computationally.

One of the significant advantages of this method is the direct use of the metric function to construct the potential, bypassing the aforementioned concerns. Utilizing the equatorial plane for the vector field (ϕ), analogous to the Poincaré plane, and the resultant dimensional reduction is another notable benefit. Ultimately, the ability to study a broader scope of the space surrounding an ultra-compact object is a fundamental point that leads to the classification of this space based on this method. Finally, a practical concept can also be introduced using this method, which we called the possible radius limit for the photon sphere.

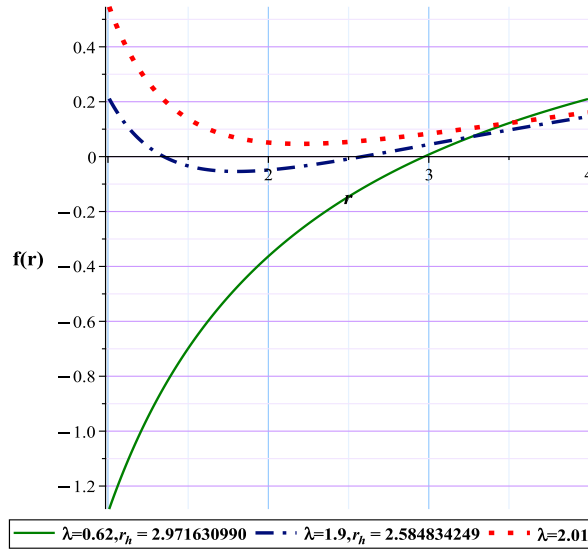
R_{PLPS}: According to the allowed range of parameters to preserve the black hole structure, we called the minimum or maximum possible radius for the appearance of an unstable photon sphere as the *R_{PLPS}*.

However, there are essential drawbacks to consider. Since the vector field (ϕ) needs to be separable with respect to spatial coordinates, only diagonal metrics with spherical symmetry can be employed. Given that most studied models possess a spherical structure, and the remainder can often be expressed in diagonal form using the C-metric, this limitation can be somewhat overlooked. Another issue is that since the Poincaré plane is used for dimensional reduction, this method may not be applicable to models with fewer than four dimensions. Finally, as this is a nascent approach, there may be weaknesses that will become apparent over time. As a

point of interest at the conclusion of this section, it should be noted that the simplifications, computational power, and the novelty of this method and mathematical model for studying the symmetric potential functions have garnered such attention that the mathematical structure of the model has been extended to thermodynamics. Consequently, extensive studies based on the mathematical model of this method have been conducted on the phase transition of black hole models [30–38].

4.1 Photon Sphere and perfect fluid dark matter black hole(PFDM)

Cosmological calculations show that the surrounding universe contains %73 dark energy, %23 dark matter, and the rest consists of baryonic matter [39–41]. This issue has been confirmed, to some extent, by baryonic sound oscillations, cosmic microwave background, weak lensing and other possible methods. Also, astrophysical observations show that massive black holes, surrounded by huge halos of dark matter, are located in the centers of giant spiral and elliptical galaxies. These evidences can be acceptable reasons for the fact that we should pay more attention to black hole solutions in the presence of dark matter and dark energy [42–46]. For this purpose, we chose the model four-dimensional PFDM [47], the metric for such black hole is



(a)

Figure 4: Metric function with different λ for PFDM black hole model

$$f = 1 - \frac{2M}{r} - \frac{\lambda \ln(\frac{r}{\lambda})}{r}, \quad (20)$$

where M is mass and λ is the parameter of intensity of PFDM. Also, we have,

$$f(r) = g(r), \quad (21)$$

$$h(r) = r, \quad (22)$$

From Eq(15) for potential and with respect to above equations we have:

$$H = \frac{\sqrt{1 - \frac{2M}{r} - \frac{\lambda \ln(\frac{r}{\lambda})}{r}}}{\sin(\theta) r}. \quad (23)$$

With respect to(21),(22) and from equation (16), we will have:

$$\phi^r = \frac{(3 \ln(\frac{r}{\lambda}) \lambda + 6M - 2r - \lambda) \csc(\theta)}{2r^3}, \quad (24)$$

$$\phi^\theta = -\frac{\sqrt{1 - \frac{2M}{r} - \frac{\lambda \ln(\frac{r}{\lambda})}{r}} \cos(\theta)}{\sin(\theta)^2 r^2}. \quad (25)$$

Case I: TTC =-1

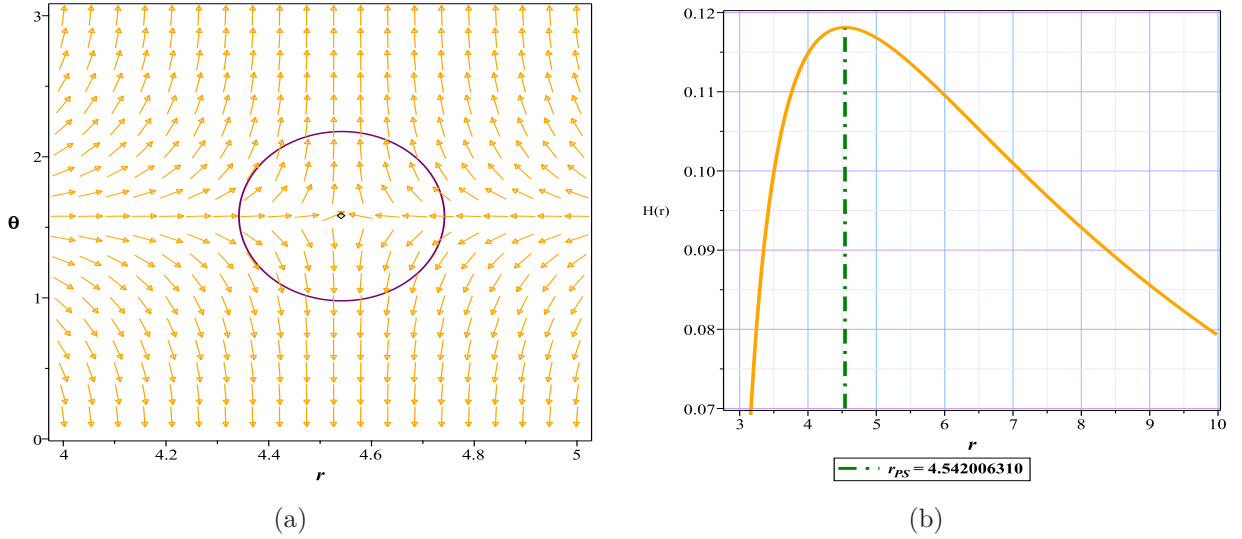


Figure 5: Fig (5a):The normal vector field n in the $(r - \theta)$ plane. The photon sphere is located at $(r, \theta) = (4.542006310, 1.57)$ with respect to $(\lambda = 0.62, M = 1)$, (5b): the topological potential $H(r)$ for PFDM black hole model

In the first case, considering the chosen value of the parameter $\lambda = 0.62$ and the presence of the event horizon ($r_h = 2.97163$) Fig (4), we observe the appearance of a photon sphere outside the event horizon. This photon sphere possesses a topological charge of -1 Fig (5a) and, as evident in Fig (5b), represents an energy maximum. Consequently, in this case, we are confronted with a black hole that contains an unstable photon sphere. However, in the second case, our choice of $\lambda = 2.15$ results in a metric function without roots, which is clearly visible in Fig (4). The gravitational structure displays two photon sphere with charges of -1 and +1, indicating a space-time with a TTC of zero, Fig (6a). Energy-wise, this situation is equivalent to the emergence of both a minimum and a maximum, as shown in Fig (6b). Since the created minimum prevents even photons from escaping such a space, observationally, the space is completely dark. Moreover, since there is no event horizon, it can be assumed that we are dealing with conditions similar to those inside an event horizon. Given these conditions, in this scenario, the structure manifests itself in the form of a naked singularity. Now we have to answer the question that for what values of the parameter λ the space will be in the form of a black hole, and for any value outside this range, will our gravitational structure correspond to a naked singularity? We have shown the answers to these questions in Table 1.

Case II: TTC = 0

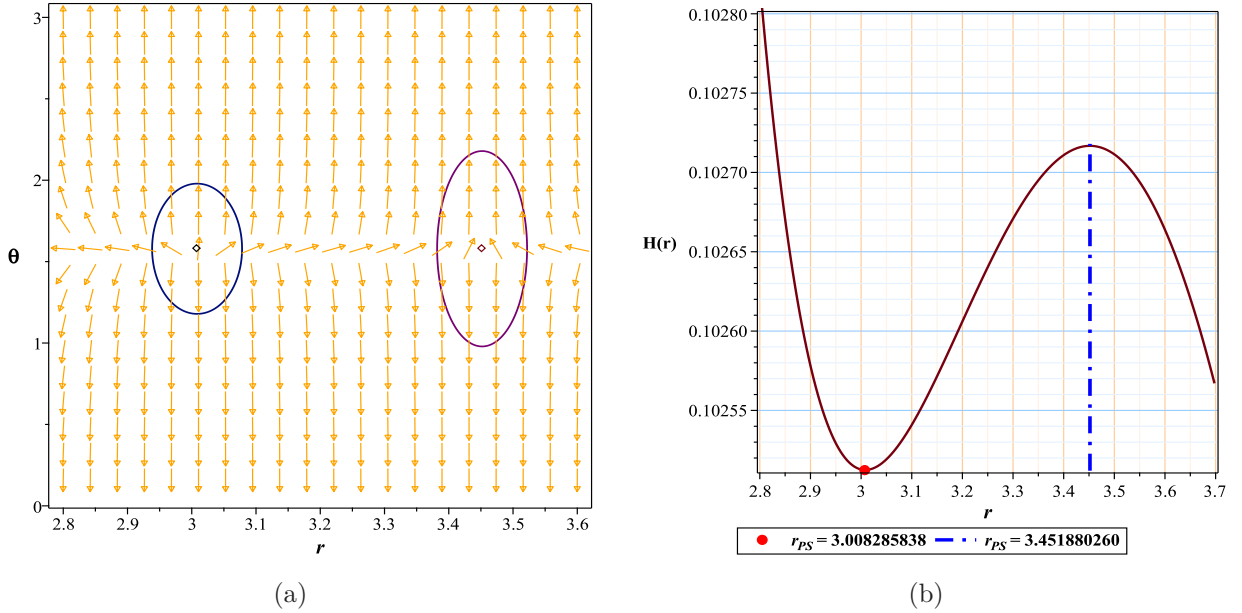


Figure 6: Fig (6a):The normal vector field n in the $(r - \theta)$ plane. The photon spheres are located at $(r, \theta) = (3.008285838, 1.57)$ and $(r, \theta) = (3.451880260, 1.57)$ with respect to $(\lambda = 2.15, M = 1)$, (6b): the topological potential $H(r)$ for PFDM black hole model

PFDM black holes	Fix parametes	Conditions	*TTC	(R_{PLPS})
*Unauthorized area	$M = 1$	$\lambda \leq 0, \lambda > 2.1554784$	<i>nothing</i>	–
unstable photon sphere	$M = 1$	$0 < \lambda < 2$	–1	2.019966202
naked singularity	$M = 1$	$2 < \lambda \leq 2.1554784$	0	–

Table 1: *Unauthorized region: is the region where the roots of ϕ equations become negative or imaginary in this region

TTC: *Total Topological Charge

Here it is necessary to note that we have focused on the domain of λ and assigned an arbitrary value to M. Obviously, changing these values can change our parameter range.

4.2 Photon Sphere and charged AdS black hole with perfect fluid dark matter(CPFDM)

In order to observe the effects of adding the electric field and the AdS radius to the action of the PDFM model on the sphere-topological photon structure, this time we go to the CPFDM model in the AdS form [48].The metric for such black hole is

$$f(r) = 1 - \frac{2m}{r} + \frac{q^2}{r^2} + \frac{r^2}{l^2} + \frac{\ln(\frac{r}{\lambda}) \lambda}{r}, \quad (26)$$

where m is mass, q is charge, λ is the parameter of intensity of PFDM, and l is the AdS radius length.

With respect to(21),(22) and from equations (15) and (16), we will have:

$$H = \frac{\sqrt{1 - \frac{2m}{r} + \frac{q^2}{r^2} + \frac{r^2}{l^2} + \frac{\ln(\frac{r}{\lambda}) \lambda}{r}}}{\sin(\theta) r}, \quad (27)$$

$$\phi^r = \frac{(-3 \ln(\frac{r}{\lambda}) \lambda r - 2r^2 + (6m + \lambda) r - 4q^2) \sqrt{1 - \frac{2m}{r} + \frac{q^2}{r^2} + \frac{r^2}{l^2} + \frac{\ln(\frac{r}{\lambda}) \lambda}{r}}}{2 \sqrt{\frac{\ln(\frac{r}{\lambda}) \lambda r l^2 + (-2mr + q^2 + r^2) l^2 + r^4}{r^2 l^2}} r^4 \sin(\theta)}, \quad (28)$$

$$\phi^\theta = -\frac{\sqrt{1 - \frac{2m}{r} + \frac{q^2}{r^2} + \frac{r^2}{l^2} + \frac{\ln(\frac{r}{\lambda})\lambda}{r}}}{\sin(\theta)^2 r^2} \cos(\theta). \quad (29)$$

Here, we have focused on λ and assigned arbitrary values to m , l , and q . It is clear that changing these values can cause a change in our parameter range.

As it is evident from table (2), the forbidden regions are located next to the allowed regions and for this black hole there is practically no region that is equivalent to the naked singularity in terms of total topological charges. As seen in Figs (7a) and (7b), the structure for two different values of λ shows the behavior of a normal black hole with a total charge of -1 and an unstable photon sphere, which is confirmed with a maximum energy. In comparison with the results from the previous state, it appears that the addition of an electric field and the AdS radius to the action has diminished the impact of the PDFM term. This is because changes in the λ parameter, which previously led to the emergence of energy minima beyond the event horizon and drove the model towards a naked singularity, now have no effect.

We became curious to know whether this effect was more a result of the presence of the electric field or the de Sitter radius. Consequently, we investigated a scenario that included only the electric field [49]. Our studies indicated that the outcomes of the new model are entirely consistent with the results of this scenario. It seems that the addition of an electric field to the model, within the normal range of electric charge, i.e., ($q/m \leq 1$) and not in extreme cases, eliminates the possibility of enhancing gravity by generating potential minima beyond the event horizon. However, since the graphical results with these obtained states were almost identical, we refrained from including them in the article to avoid confusion and excessive volume.

CPFDM black holes	Fix parametes	Conditions	*TTC
*Unauthorized area	$q = 0.1, m = 1, l = 1$	$\lambda < 0$	<i>nothing</i>
unstable photon sphere	$q = 0.1, m = 1, l = 1$	$0 < \lambda$	-1

Table 2: *Unauthorized region: is the region where the roots of ϕ equations become negative or imaginary in this region.

TTC: *Total Topological Charge

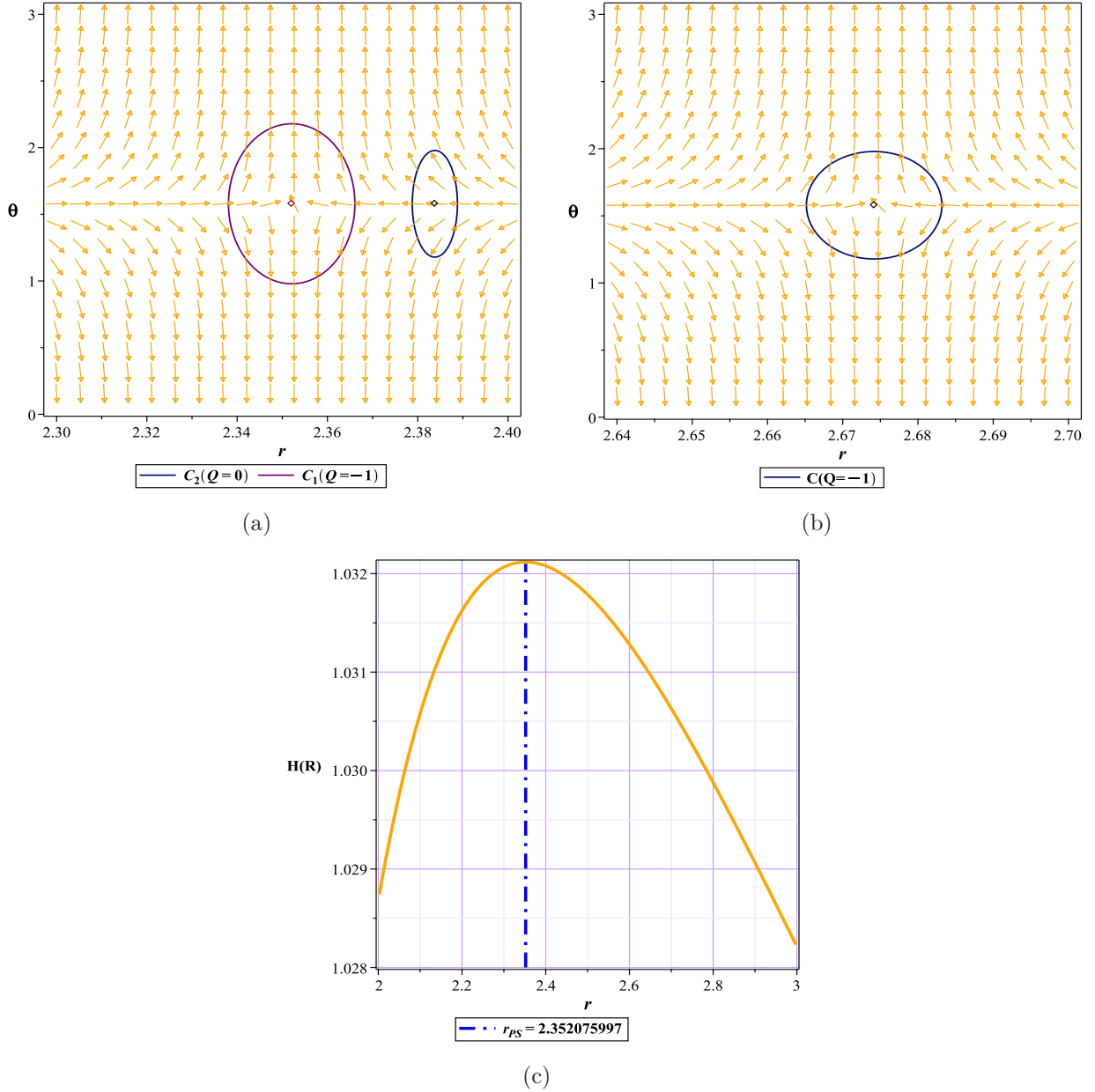


Figure 7: The normal vector field n in the $(r - \theta)$ plane. The photon spheres are located at $(r, \theta) = (2.352075997, 1.57)$ for fig (7a) with respect to $(q = 0.1, m = 1, \lambda = 0.2, l = 1)$ and $(r, \theta) = (2.674176616, 1.57)$, for fig (7b) with respect to $(q = 0.1, m = 1, \lambda = 1.69, l = 1)$, (7c): the topological potential $H(r)$ for CPFDM black hole model

4.3 Photon Sphere and Euler-Heisenberg black hole

The Euler-Heisenberg black hole is a type of black hole that has a nonlinear electromagnetic field due to quantum effects. In fact, Euler and Heisenberg developed an effective Lagrangian for quantum electrodynamics (QED) that described the interaction of photons with each other in the presence of a strong electromagnetic field [50]. Casimir and Polder applied Euler-Heisenberg Lagrangian to the problem of a charged black hole in general relativity. They found that QED corrections affect the electromagnetic field, thermodynamics and stability of black hole. They named this black hole Euler-Heisenberg black hole and showed that it has interesting properties.

- The QED parameter, which measures the strength of the nonlinear effects, can be positive or negative. A positive QED parameter reduces the electric field near the horizon and increases the mass of the black hole, while a negative QED parameter enhances the electric field and decreases the mass [51].
- The QED parameter also influences the existence and location of the inner and outer horizons of the black hole. For a positive QED parameter, there is always a single horizon, while for a negative QED parameter, there can be two horizons, one horizon, or no horizon at all, depending on the values of the mass and charge [51].
- The QED parameter also modifies the stability of the black hole against perturbations. For a positive QED parameter, the black hole is stable for any mass and charge, while for a negative QED parameter, there is a range of mass and charge where the black hole is unstable and can decay into radiation or smaller black holes [52].

Euler Heisenberg's spherical four-dimensional black hole has a metric function in the following form [53]:

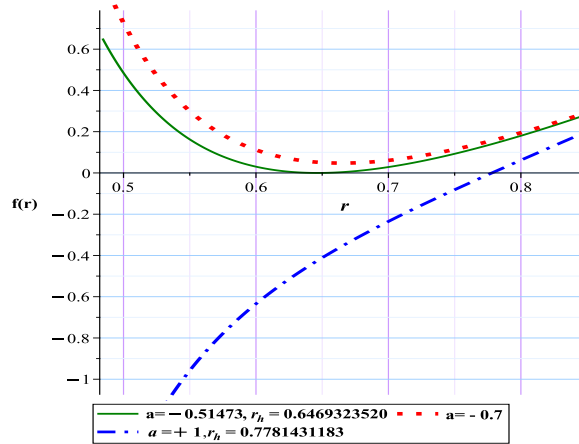


Figure 8: Metric function with different a for Euler-Heisenberg black hole model

$$f(r) = 1 - \frac{2m}{r} + \frac{q^2}{r^2} + \frac{r^2}{l^2} - \frac{aq^4}{20r^6}, \quad (30)$$

where parameter m is the ADM mass, q is the electric charge and "a" represents the strength of the QED correction. With respect to(21),(22) and from equations (15) and (16), we will have,

$$H = \frac{\sqrt{100 - \frac{200m}{r} + \frac{100q^2}{r^2} + \frac{100r^2}{l^2} - \frac{5q^4a}{r^6}}}{10 \sin(\theta) r}, \quad (31)$$

$$\phi^r = \frac{(30.0r^5 - 12.8r^4 + 0.8192a - 10.0r^6) \sqrt{100 - \frac{200m}{r} + \frac{100q^2}{r^2} + \frac{100r^2}{l^2} - \frac{5q^4a}{r^6}}}{10r^8 \sin(\theta) \sqrt{\frac{(100.0r^6 - 200.0r^5 + 64.0r^4 - 2.048a)l^2 + 100.0r^8}{r^6 l^2}}}, \quad (32)$$

$$\phi^\theta = -\frac{\sqrt{\frac{(-200r^5m + 100r^4q^2 + 100r^6 - 5q^4a)l^2 + 100r^8}{l^2 r^6}} \cos(\theta)}{10 \sin(\theta)^2 r^2}. \quad (33)$$

Case I: TTC =-1

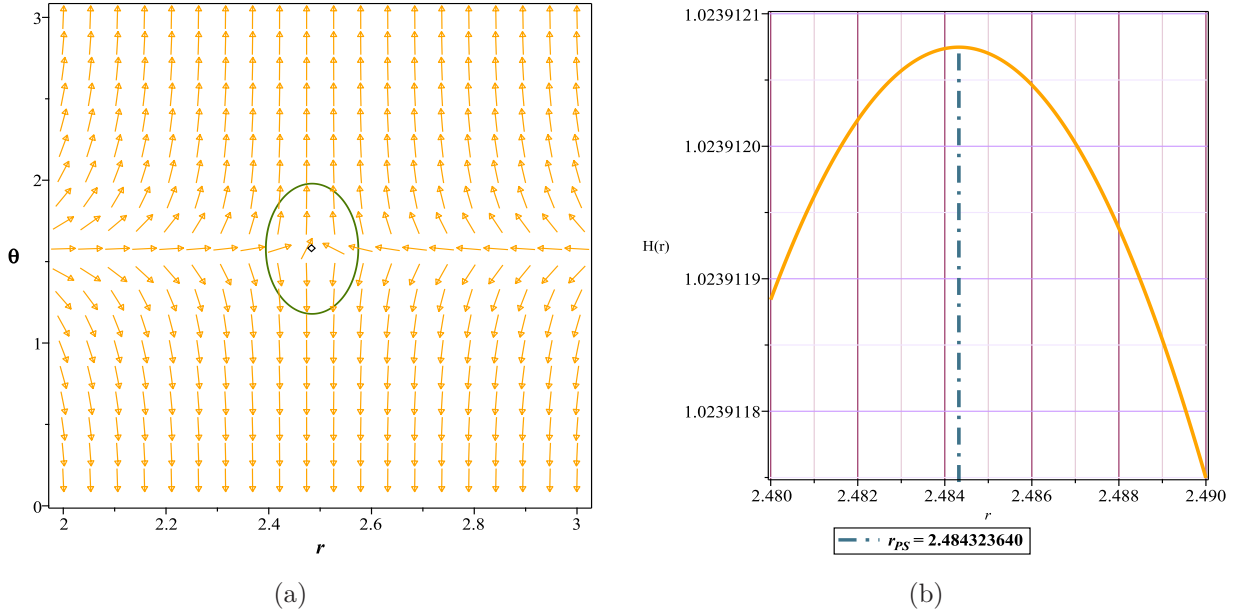


Figure 9: The normal vector field n in the $(r - \theta)$ plane. The photon spheres are located at $(r, \theta) = (2.484328812, 1.57)$ for fig (9a) with respect to $(q = 0.8, m = 1, a = -0.51473, l = 1)$, fig (9b) the topological potential $H(r)$ for Euler-Heisenberg black hole model

Case II: $TTC = 0$

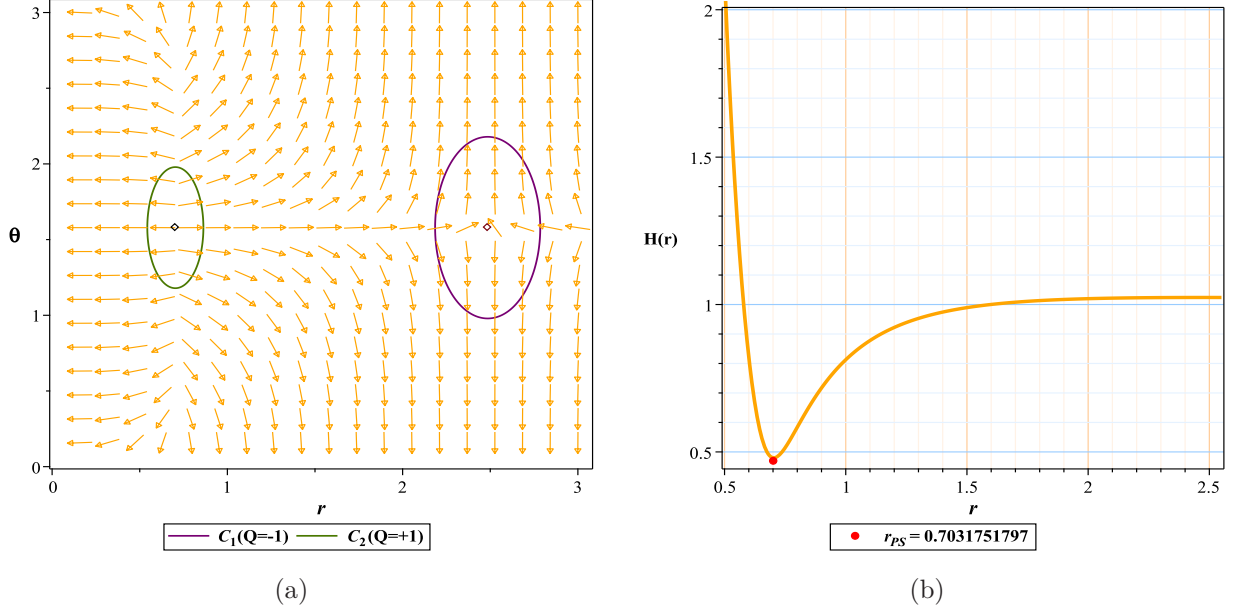


Figure 10: The normal vector field n in the $(r - \theta)$ plane. The photon spheres are located at $(r, \theta) = (0.7031751797, 1.57)$, $(r, \theta) = (2.483792443, 1.57)$ for fig (10a) with respect to $(q = 0.8, m = 1, a = -1, l = 1)$, fig (10b) the topological potential $H(r)$ for Euler-Heisenberg black hole model

We have focused on parameter a , for this purpose we have considered an arbitrary value for mass and charge ($m = 1, q = 0.8$). As we can see in Figs (8),(9),(10), our chosen range for a can lead to different behaviors for the photon sphere. For example, Fig (9a), with a topological charge of -1, indicates a normal black hole behavior, it means that we have an unstable photon sphere. Conversely, in Fig (10b), the appearance of a minimum in the space without an event horizon and the zero TTC fig (10a) all imply the existence of a naked singularity. Based on this, the following intervals can be used to have different modes (table3).

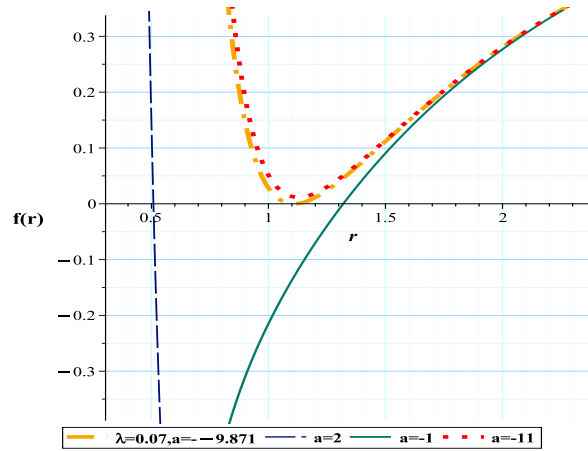
Euler-Heisenberg-AdS black holes	Fix parametes	Conditions	*TTC	(R_{PLPS})
*Unauthorized area	$q = 0.8, m = 1, l = 1$	$a < -144.87$	<i>nothing</i>	–
naked singularity	$q = 0.8, m = 1, l = 1$	$-144.87 < a < -0.51473$	0	–
unstable photon sphere	$q = 0.8, m = 1, l = 1$	$a \geq -0.51473$	-1	2.484323651

Table 3: *Unauthorized region: is the region where the roots of ϕ equations become negative or imaginary in this region

TTC: *Total Topological Charge

4.4 Photon Sphere and Euler-Heisenberg black hole surrounded by PFDM

In order to observe the effects of adding the PFDM to the action of the Euler-Heisenberg model on the sphere-topological photon structure, this time we go to the Euler-Heisenberg black hole surrounded by PFDM model [54]. The metric for such black hole is:



(a)

Figure 11: Metric function with different a for Euler-Heisenberg black hole surrounded by PFDM

$$f = 1 - \frac{2m}{r} + \frac{q^2}{r^2} - \frac{aq^4}{20r^6} + \frac{\lambda \ln\left(\frac{r}{\lambda}\right)}{r}, \quad (34)$$

where parameter m is the ADM mass, q is the electric charge, λ is the parameter of intensity of PFDM and "a" represents the strength of the QED correction. With respect to (21), (22) and from equations (15) and (16), we will have,

$$H = \frac{\sqrt{100 - \frac{200m}{r} + \frac{100q^2}{r^2} - \frac{5aq^4}{r^6} + \frac{100\lambda \ln\left(\frac{r}{\lambda}\right)}{r}}}{10r \sin(\theta)}, \quad (35)$$

$$\phi^r = -\frac{(15\lambda \ln\left(\frac{r}{\lambda}\right) r^5 - 5\lambda r^5 - 30m r^5 + 20q^2 r^4 + 10r^6 - 2aq^4) \csc(\theta)}{10r^8}, \quad (36)$$

$$\phi^\theta = -\frac{\sqrt{100 - \frac{200m}{r} + \frac{100q^2}{r^2} - \frac{5aq^4}{r^6} + \frac{100\lambda \ln\left(\frac{r}{\lambda}\right)}{r}} \cos(\theta)}{10r^2 \sin(\theta)^2}. \quad (37)$$

Case I: TTC = -1

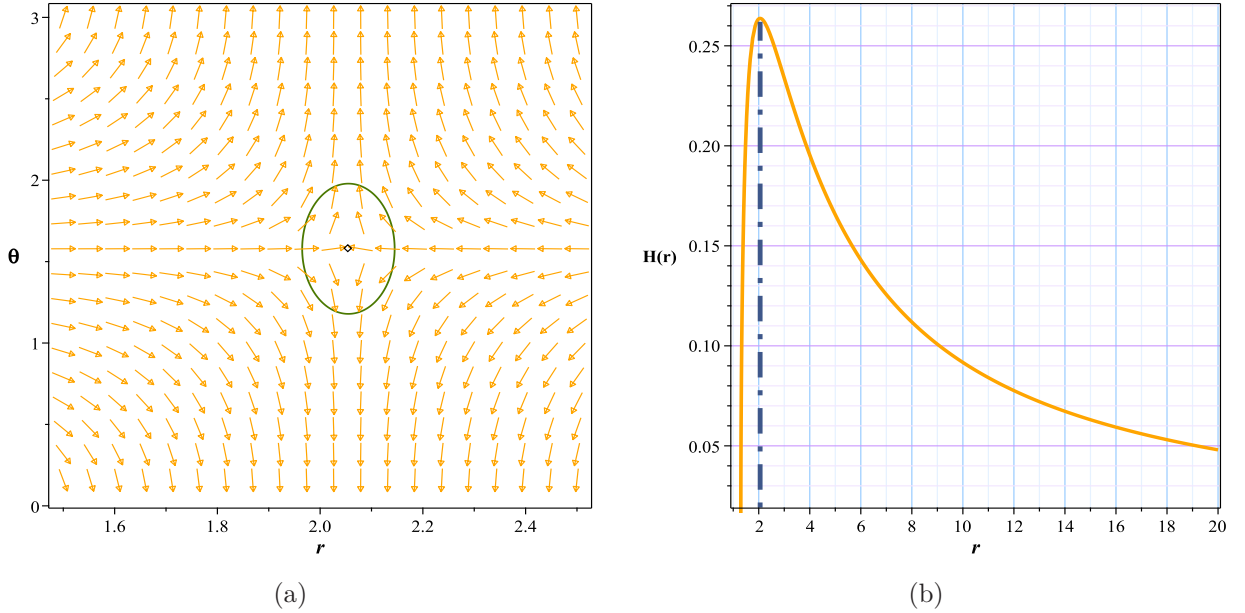


Figure 12: The normal vector field n in the $(r - \theta)$ plane. The photon spheres are located at $(r, \theta) = (2.055057, 1.57)$ for fig (12a) with respect to $(q = 0.8, m = 1, a = -0.51473, l = 1, \lambda = 0.07)$, fig (12b) the topological potential $H(r)$ for Euler-Heisenberg black hole surrounded by PFDM model

Case II: $TTC = 0$

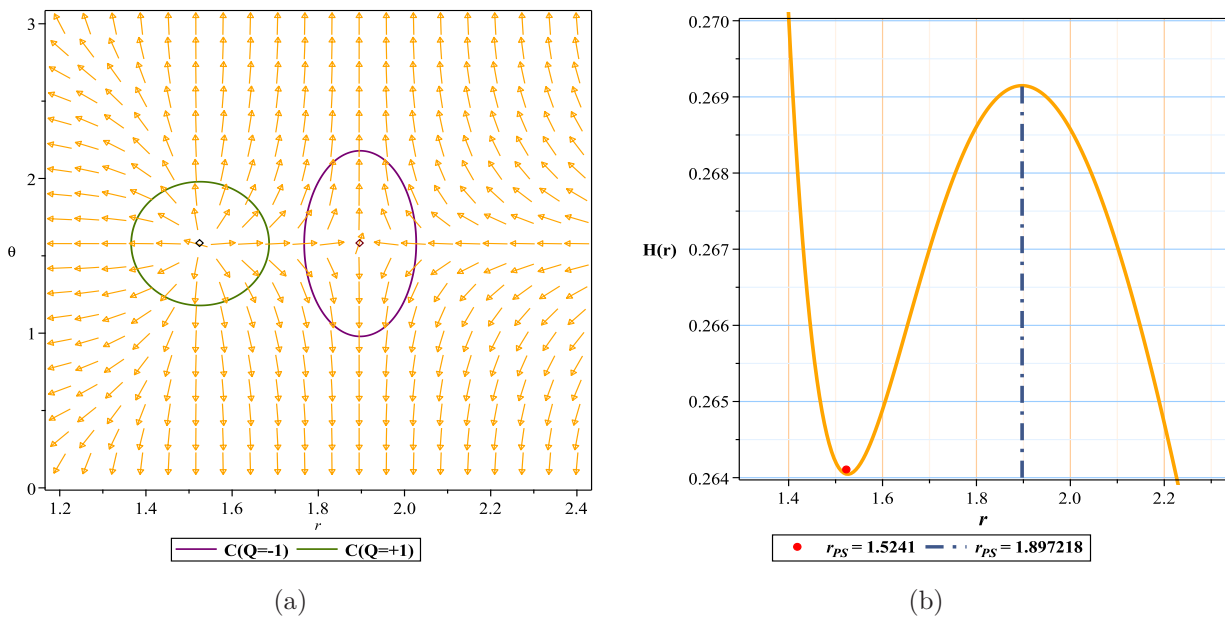


Figure 13: The normal vector field n in the $(r - \theta)$ plane. The photon spheres are located at $(r, \theta) = (1.5241, 1.57)$, $(r, \theta) = (1.897218, 1.57)$ for fig (13a) with respect to $(q = 0.8, m = 1, a = -1, l = 1, \lambda = 0.07)$, fig (13b) the topological potential $H(r)$ for Euler-Heisenberg black hole surrounded by PFDM model

Regardless of the impact of the AdS radius, which we have admittedly examined to a lesser extent in this article, it is evident from the comparison of the results in Tables 4 and 5 with Table 3 that the addition of PFDM to the model has caused a significant increase in the range affected by black hole behavior. Given the negative value of the parameter (a), which signifies a greater influence of the electric field, it appears that when dark matter is absent from the model (as shown in Table 3), even very small values of (a) rapidly expand the domain of gravitational dominance. Consequently, a gravitational minimum emerges swiftly beyond the event horizon, leading to the model's becoming a naked singularity. As observed (in table 3), the domain of dominance of this naked singularity is significantly extensive due to the increase in the parameter within a considerably large negative range. However, in the presence of dark matter (as indicated in Tables 4 and 5), this structure seems to act as a reverse agent, preventing the rapid growth and expansion of the model's gravitational domain. Thus, as evident, we maintain the conditions for the existence of a black hole with an unstable photon sphere over a substantial range of negative (a) values, In other words, it appears that the inclusion of dark

matter has somewhat prevented the formation of gravitational minima over a larger range, which is an intriguing effect.

Euler-Heisenberg PFDM black holes	Fix parametes	Conditions	*TTC	(R_{PLPS})
*Unauthorized area	$q = 0.8, m = 1, \lambda = 0.07$	$a < -40$	<i>nothing</i>	–
naked singularity	$q = 0.8, m = 1, \lambda = 0.07$	$-39 \leq a < -9.872$	0	–
unstable photon sphere	$q = 0.8, m = 1, \lambda = 0.07$	$a \geq -9.871$	–1	2.026241903

Table 4: *Unauthorized region: is the region where the roots of ϕ equations become negative or imaginary in this region

TTC: *Total Topological Charge

Euler-Heisenberg PFDM black holes	Fix parametes	Conditions	*TTC	(R_{PLPS})
*Unauthorized area	$q = 0.8, m = 1, \lambda = 0.6$	$a < -14.9$	<i>nothing</i>	–
naked singularity	$q = 0.8, m = 1, \lambda = 0.6$	$-14.9 < a < -4.21$	0	–
unstable photon sphere	$q = 0.8, m = 1, \lambda = 0.6$	$a \geq -4.2$	–1	1.583699320

Table 5: *Unauthorized region: is the region where the roots of ϕ equations become negative or imaginary in this region

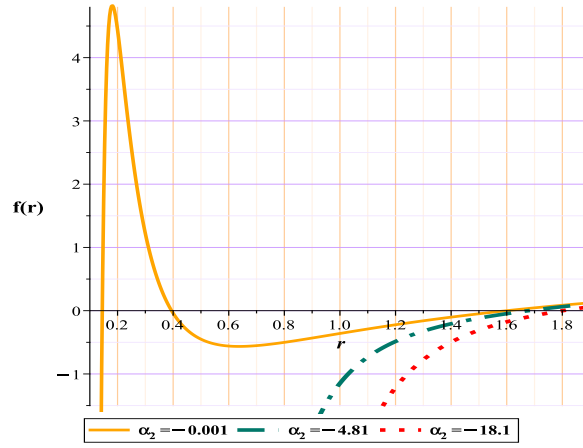
TTC: *Total Topological Charge

4.5 Photon Sphere and Black Holes With Nonlinear Electrodynamics(NLE)

The idea that nonlinear electrodynamics might be able to solve the problem of black hole singularities led to many studies to find regular solutions, which led to black holes such as "Bardeen" [55] or "Ayon-Beat-Garcia" [56, 57]. As the last model we chose for our work, we went to a black hole that was selected by "Gao" [58] to investigate the effects of nonlinear electrodynamics and the possibility that a black hole can have more than two event horizons. We study this black hole in three and four-horizon states, and we will show that additional studies confirm the results of the mentioned article in three-horizon states.

Three-Horizons mode

So, according to [58] for the metric function in the case of three-horizons, we will have



(a)

Figure 14: Metric function with different α for NLE model

$$f = 1 - \frac{2m}{r} + \frac{q^2}{r^2} + \frac{2q^4\alpha_2}{5r^6}, \quad (38)$$

here α_2 are dimensional constants, m is mass and q is charge, With respect to (21), (22) and from equations (15) and (16), we will have

$$H = \frac{\sqrt{25 - \frac{50M}{r} + \frac{25q^2}{r^2} + \frac{10q^4\alpha_2}{r^6}}}{5 \sin(\theta) r}, \quad (39)$$

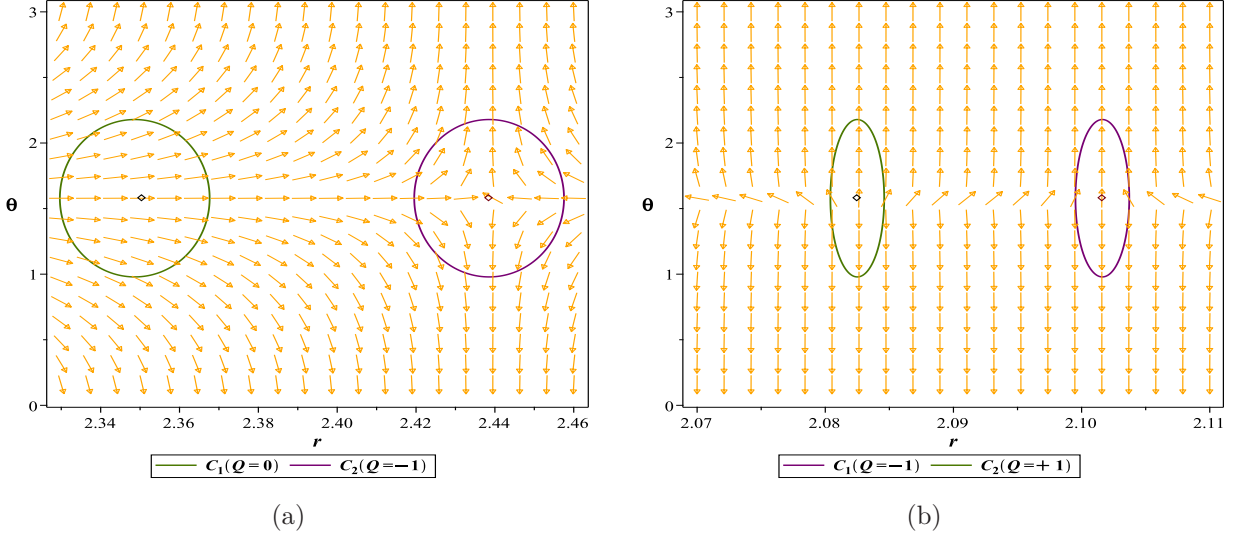


Figure 15: The normal vector field n in the $(r - \theta)$ plane. The photon spheres are located at $(r, \theta) = (2.438537647, 1.57)$ for fig (6a) with respect to $(q = 0.8, m = 1, \alpha_2 = -4.81,)$ and $(r, \theta) = (2.082498057, 1.57), (r, \theta) = (2.101619064, 1.57)$ for fig (6b) with respect to $(q = 0.8, m = 1, \alpha_2 = -18.1,)$

$$\phi^r = \frac{(15M r^5 - 10q^2 r^4 - 5r^6 - 8q^4 \alpha_2) \sqrt{25 - \frac{50M}{r} + \frac{25q^2}{r^2} + \frac{10q^4 \alpha_2}{r^6}}}{5 \sqrt{\frac{-50M r^5 + 25q^2 r^4 + 25r^6 + 10q^4 \alpha_2}{r^6}} r^8 \sin(\theta)}, \quad (40)$$

$$\phi^\theta = -\frac{\sqrt{25 - \frac{50M}{r} + \frac{25q^2}{r^2} + \frac{10q^4 \alpha_2}{r^6}} \cos(\theta)}{5 \sin(\theta)^2 r^2}. \quad (41)$$

The results of "Gao's" work on the black hole showed that to have three horizons, we need $\alpha_2 < 0$. It should be stated that our results confirm the above-mentioned limit for black hole behavior. Our results show that for $\alpha_2 \leq 4.8148$, the model shows the behavior of a regular black hole and has an unstable photon sphere, Figs (6a). For the range between $4.8148 < \alpha_2 < 18.1064$ the behavior of the model is the naked singularity, Figs (6b) and for a limit greater than that, the system lacks any spherical photon structure, either stable or unstable, and practically, it will most likely lack a black hole structure table(6). Since the structure of the energy diagrams was similar to the past behaviors, we refrained from displaying them here.

NLE black holes(Three-horizons mode)	Fix parametes	Conditions	*TTC	(R_{PLPS})
unstable photon sphere	$q = 0.8, m = 1$	$\alpha_2 \leq 4.8148$	-1	2.438486243
naked singularity	$q = 0.8, m = 1$	$4.8148 < \alpha_2 < 18.1064$	0	-
*Unauthorized area	$q = 0.1, m = 8$	$18.1064 < \alpha_2$	<i>nothing</i>	-

Table 6: *Unauthorized region: is the region where the roots of ϕ equations become negative or imaginary in this region.

TTC: *Total Topological Charge

Four-Horizons mode

It seems that "Gao" in this article [58] did not mention the allowed distances in the case of 4 horizons and selected the parameters based on the need and in an optional way. But we show that in this case, there can be meaningful and meaningless intervals for our choice table(7).

Unlike all previous shapes, in this case another parameter has been added to our equations. This means that, since we have only one condition to establish, so our restrictions are increased, and we have to give a value to one of the parameters and add it to our constants table, but this will not reduce the efficiency of our method.

Because, foremost, this condition protects us from being unaware of the parameters of the system and their limitations, and at least it is always possible to make a decision about the allowed ranges of one of the parameters with good accuracy.

Secondly, this optionally of parameter selection will leave our hands free to include the less effective parameter in our constants table according to the selection conditions. According to [58] for the metric function in the case of four-horizons, we will have

$$f(r) = 1 - \frac{2m}{r^2} + \frac{q^2}{r^2} + \frac{2q^4\alpha_2}{5r^6} + \frac{q^6(16\alpha_2^2 - 4\alpha_3)}{9r^{10}}, \quad (42)$$

here α_i are dimensional constants, m is mass and q is charge, with respect to (21), (22) and from equations (15) and (16), we will have:

$$H = \frac{\sqrt{225 - \frac{450m}{r^2} + \frac{225q^2}{r^2} + \frac{90q^4\alpha_2}{r^6} + \frac{25q^6(16\alpha_2^2 - 4\alpha_3)}{r^{10}}}}{15 \sin(\theta) r}, \quad (43)$$

$$\phi^r = \frac{-15r^{10} + (-30q^2 + 60m)r^8 - 24q^4\alpha_2r^4 - 160q^6\left(\alpha_2^2 - \frac{\alpha_3}{4}\right)}{15r^{12}\sin(\theta)}, \quad (44)$$

$$\phi^\theta = -\frac{\sqrt{225 - \frac{450m}{r^2} + \frac{225q^2}{r^2} + \frac{90q^4\alpha_2}{r^6} + \frac{25q^6(16\alpha_2^2 - 4\alpha_3)}{r^{10}}}}{15\sin(\theta)^2 r^2} \cos(\theta). \quad (45)$$

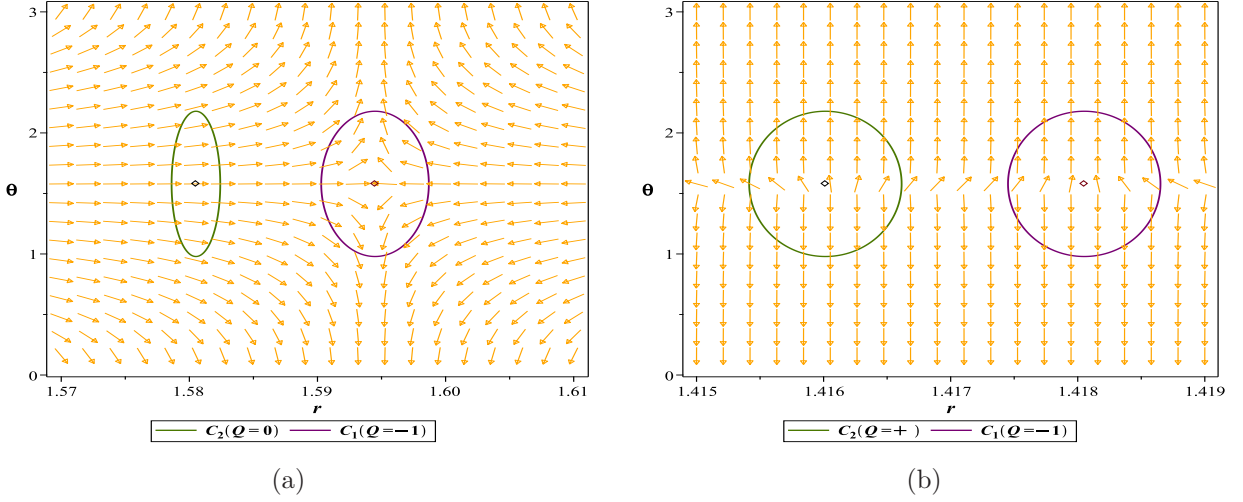


Figure 16: The normal vector field n in the $(r - \theta)$ plane. The photon spheres are located at $(r, \theta) = (1.594492202, 1.57)$ for fig (7a) with respect to $(q = 0.9, m = 1, \alpha_2 = -1, \alpha_3 = 4)$ and $(r, \theta) = (1.416014166, 1.57), (r, \theta) = (1.418051264, 1.57)$ for fig (7b) with respect to $(q = 0.9, m = 1, \alpha_2 = -1, \alpha_3 = -3.2541)$

NLE black holes(4-horizons mode)	Fix parametes	Conditions	*TTC	(R_{PLPS})
*Unauthorized area	$q = 0.9, m = 1, \alpha_2 = -1$	$\alpha_3 < -3.2543$	<i>nothing</i>	–
naked singularity	$q = 0.9, m = 1, \alpha_2 = -1$	$-3.2543 < \alpha_3 < 3.99$	0	–
unstable photon sphere	$q = 0.9, m = 1, \alpha_2 = -1$	$4 \leq \alpha_3$	–1	1.594492202

Table 7: *Unauthorized region: is the region where the roots of ϕ equations become negative or imaginary in this region.

TTC: *Total Topological Charge

5 Conclusions

In this paper, we aim to provide a comprehensive analysis of ultra-compact objects with various gravitational structures by examining the existence and behavioral patterns of topological photon and anti-photon spheres. We approach this study by TTC and analyzing the extremums of the defined effective potential graph. The field diagrams, zero points, and effective potential graph are meticulously plotted, and the characteristics under study detailed in Tables 1-7.

Indeed, it should be noted that The ability to study the behavior of photon spheres solely through the metric function and a potential directly derived from it is a distinct advantage. Although, there are limitations due to spherical symmetry and the method's applicability to structures beyond four dimensions. But, what distinguishes this work is its unique perspective on the necessity of a photon sphere for ultra-compact gravitational structures like black holes—a necessity confirmed by numerous empirical and theoretical studies [15–20, 59–71]. Utilizing this necessity, which is essentially a bidirectional relationship between the photon sphere and the gravitational structure, can lead to several interesting implications:

- As a preliminary outcome, the calculation of topological photon spheres can complement the metric function results and even serve as a suitable replacement for that in examining the behavior of gravitational structures. An unstable photon sphere only dominates the space of the system when an event horizon exists, therefore, the range in which the behavior of the model is a black hole, practically meets the basic requirements for WCCC. Additionally, the broader coverage of the topological photon sphere over the surrounding space of the gravitational structure makes it more distinguished than the metric function.
- The most significant concept shaping the primary goal of the article is that we can easily classify the parameter space of the models under study based on the existence and location of topological photon and anti-photon spheres. This means we can precisely indicate which parameter range of the model corresponds to a black hole structure, a naked singularity, or even a model that mathematically lacks a physical and scientific response for its surrounding space, which we have termed the forbidden zone. [72]
- Based on this study, a question has arisen for us that requires further detailed examination: If we slice the space-time of an ultra-compact body (a naked singularity) with a horizontal plane, it will have at least one ring. A stable photon sphere with a total charge of 1 or two distinct rings (one stable and the other unstable) with a total charge of 0. Considering that any photon trapped in a stable ring will never leave its orbit outwardly, So practically from this border towards the center of the structure, the area becomes invisible to us. Given the vital importance of the photon sphere in determining the shadow, this ring essentially acts as an observable boundary for us. Now, since according to the WCC conjecture, anything un-

predictable must be hidden behind the event horizon, our question is whether hypothetically, the radius of the stable photon sphere can be considered a new hypothetical horizon for the space-time under study? What implications would this choice have for the structure of the ultra-compact object?

- The other achievement of this method is that we can adjust the parameters of our system in such a way that the model under study is compelled to exhibit the desired behavior, or conversely, we can estimate the approximate range of model parameters based on the presence of the photon sphere in a specific region of space. For instance, in certain gravitational studies, we require a gravitational structure that adheres to specific principles and behaviors. In such cases, where we need the model's parameters to fall within a specific range while simultaneously maintaining the structure in a defined form, such as a black hole, this method can play a significant role.

To elucidate further, in the model studying the Swampland Conjectures, there are hypotheses such as the Weak Gravity Conjecture (WGC) which necessitate that The structure under study, while being overly charged, still retains in the form of a black hole. In this work, we propose that for such scenarios, the topological behavior of the photon sphere can be utilized, and after setting the parameters as desired, the topological photon sphere can be examined to determine whether the optimal conditions can be achieved or not.

Finally, it is imperative to highlight that during the formulation of a theory, parameters are added as necessitated by the theoretical framework. These parameters may conceptually possess a defined range from the outset or be devoid of any limitations. In this article, we have endeavored to address the question of what impact these theories, when incorporated into black hole action, will have on the behavior of the photon sphere for their permissible values. Furthermore, from the perspective of the photon sphere, whether these parameters, for all their previously allowed values, will result in the natural behavior of the model under study, or if new constraints must be imposed on the parameters in the context of black hole studies.

References

- [1] Goswami, Rituparno, Pankaj S. Joshi, and Parampreet Singh. "Quantum evaporation of a naked singularity." *Physical review letters* 96.3 (2006): 031302.
- [2] Christodoulou, Demetrios. "The instability of naked singularities in the gravitational collapse of a scalar field." *Annals of Mathematics* 149.1 (1999): 183-217.
- [3] Joshi, P. S., and I. H. Dwivedi. "Naked singularities in spherically symmetric inhomogeneous Tolman-Bondi dust cloud collapse." *Physical Review D* 47.12 (1993): 5357.
- [4] Pugliese, Daniela, and Hernando Quevedo. "Naked singularities and black hole Killing horizons." *arXiv preprint arXiv:2402.07512* (2024).
- [5] Goswami, Rituparno, and Pankaj S. Joshi. "Spherical gravitational collapse in N dimensions." *Physical Review D* 76.8 (2007): 084026.
- [6] Ghosh, Avisikta. "Study of Orbital Dynamics in Singular and Regular Naked Singularity Space-times." *arXiv preprint arXiv:2401.10771* (2024).
- [7] Wang, Mingzhi, et al. "The images of a rotating naked singularity with a complete photon sphere." *arXiv preprint arXiv:2307.16748* (2023).
- [8] Joshi, Pankaj S., and Sudip Bhattacharyya. "Primordial naked singularities." *arXiv preprint arXiv:2401.14431* (2024).
- [9] Chen, Yiqian, Peng Wang, and Haitang Yang. "Observations of Orbiting Hot Spots around Naked Singularities." *arXiv preprint arXiv:2309.04157* (2023).
- [10] Virbhadra, K. S. "Naked singularities and Seifert's conjecture." *Physical Review D* 60.10 (1999): 104041. Deliyski, Valentin, et al. "Observing naked singularities by the present and next-generation Event Horizon Telescope." *arXiv preprint arXiv:2401.14092* (2024).
- [11] Viththani, Divyesh P., et al. "Particle motion and tidal force in a non-vacuum-charged naked singularity." *arXiv preprint arXiv:2402.02069* (2024).
- [12] Mosani, Karim, Dipanjan Dey, and Pankaj S. Joshi. "Strong curvature naked singularities in spherically symmetric perfect fluid collapse." *Physical Review D* 101.4 (2020): 044052.
- [13] Acharya, Kauntey, et al. "Naked Singularity as a Possible Source of Ultra-High Energy Cosmic Rays." *arXiv preprint arXiv:2303.16590* (2023).
- [14] Goswami, Rituparno, and Pankaj S. Joshi. "Gravitational collapse of an isentropic perfect fluid with a linear equation of state." *Classical and Quantum Gravity* 21.15 (2004): 3645.

- [15] Akiyama, Kazunori, et al. "First M87 event horizon telescope results. V. Physical origin of the asymmetric ring." *The Astrophysical Journal Letters* 875.1 (2019): L5.
- [16] Abbott, B. P., et al. "GWTC-1: a gravitational-wave transient catalog of compact binary mergers observed by LIGO and Virgo during the first and second observing runs." *Physical Review X* 9.3 (2019): 031040.
- [17] Abbott, Benjamin P., et al. "Observation of gravitational waves from a binary black hole merger." *Physical review letters* 116.6 (2016): 061102.
- [18] Akiyama, Kazunori, et al. "First M87 event horizon telescope results. VI. The shadow and mass of the central black hole." *The Astrophysical Journal Letters* 875.1 (2019): L6. 041301.
- [19] Event Horizon Telescope Collaboration. "First M87 event horizon telescope results. IV. Imaging the central supermassive black hole." arXiv preprint arXiv:1906.11241 (2019).
- [20] Akiyama, Kazunori, et al. "First M87 event horizon telescope results. VI. The shadow and mass of the central black hole." *The Astrophysical Journal Letters* 875.1 (2019): L6.
- [21] Cunha, Pedro VP, Carlos AR Herdeiro, and Eugen Radu. "Fundamental photon orbits: black hole shadows and spacetime instabilities." *Physical Review D* 96.2 (2017): 024039.
- [22] Carballo-Rubio, Raúl, and Astrid Eichhorn. "Black hole horizons must be veiled by photon spheres." arXiv preprint arXiv:2405.08872 (2024).
- [23] Cardoso, Vitor, et al. "Light rings as observational evidence for event horizons: long-lived modes, ergoregions and nonlinear instabilities of ultracompact objects." *Physical Review D* 90.4 (2014): 044069.
- [24] Wei, Shao-Wen. "Topological charge and black hole photon spheres." *Physical Review D* 102.6 (2020): 064039.
- [25] Sadeghi, Jafar, et al. "Thermodynamic topology and photon spheres in the hyperscaling violating black holes." *Astroparticle Physics* 156 (2024): 102920.
- [26] Cunha, Pedro VP, and Carlos AR Herdeiro. "Stationary black holes and light rings." *Physical Review Letters* 124.18 (2020): 181101.
- [27] Cunha, Pedro VP, Emanuele Berti, and Carlos AR Herdeiro. "Light-ring stability for ultracompact objects." *Physical review letters* 119.25 (2017): 251102.

- [28] A Poincaré section is a lower-dimensional subspace of the state space of a continuous dynamical system that intersects a periodic orbit transversally and maps the points of intersection as a discrete dynamical system.
- [29] Y. S. Duan, The structure of the topological current, SLAC-PUB-3301, (1984).
- [30] Sadeghi, Jafar, et al. "Bardeen black hole thermodynamics from topological perspective." *Annals of Physics* 455 (2023): 169391.
- [31] Alipour, Mohammad Reza, et al. "Topological classification and black hole thermodynamics." *Physics of the Dark Universe* 42 (2023): 101361.
- [32] Sadeghi, Jafar, et al. "Thermodynamic topology of black holes from bulk-boundary, extended, and restricted phase space perspectives." *Annals of Physics* 460 (2024): 169569.
- [33] Sadeghi, Jafar, et al. "Bulk-boundary and RPS Thermodynamics from Topology perspective." arXiv preprint arXiv:2306.16117 (2023).
- [34] Sadeghi, J., et al. "Topology of Hayward-AdS black hole thermodynamics." *Physica Scripta* 99.2 (2024): 025003.
- [35] Wu, Di. "Classifying topology of consistent thermodynamics of the four-dimensional neutral Lorentzian NUT-charged spacetimes." *The European Physical Journal C* 83.5 (2023): 365.
- [36] Wu, Di. "Consistent thermodynamics and topological classes for the four-dimensional Lorentzian charged Taub-NUT spacetimes." *The European Physical Journal C* 83.7 (2023): 589.
- [37] Wu, Di. "Topological classes of thermodynamics of the four-dimensional static accelerating black holes." *Physical Review D* 108.8 (2023): 084041.
- [38] Wu, Di. "Topological classes of rotating black holes." *Physical Review D* 107.2 (2023): 024024.
- [39] Lonappan, Anto I., et al. "Bayesian evidences for dark energy models in light of current observational data." *Physical Review D* 97.4 (2018): 043524. (2009): 195011.
- [40] Ade, Peter AR, et al. "Planck 2013 results. I. Overview of products and scientific results." *Astronomy , Astrophysics* 571 (2014): A1.
- [41] Carroll, Sean M. *Dark Matter, Dark Energy: The Dark Side of the Universe*. Parts 1 , 2. Teaching Company, 2007.

- [42] Rubin, Vera C., W. Kent Ford Jr, and Norbert Thonnard. "Rotational properties of 21 SC galaxies with a large range of luminosities and radii, from NGC 4605/R= 4kpc/to UGC 2885/R= 122 kpc." *Astrophysical Journal, Part 1*, vol. 238, June 1, 1980, p. 471-487. 238 (1980): 471-487.
- [43] Persic, Massimo, Paolo Salucci, and Fulvio Stel. "The universal rotation curve of spiral galaxies—I. The dark matter connection." *Monthly Notices of the Royal Astronomical Society* 281.1 (1996): 27-47.
- [44] Akiyama, Kazunori, et al. "First M87 event horizon telescope results. VI. The shadow and mass of the central black hole." *The Astrophysical Journal Letters* 875.1 (2019): L6.
- [45] Event Horizon Telescope Collaboration. "First M87 event horizon telescope results. IV. Imaging the central supermassive black hole." arXiv preprint arXiv:1906.11241 (2019).
- [46] Bertone, Gianfranco, and Dan Hooper. "History of dark matter." *Reviews of Modern Physics* 90.4 (2018): 045002.
- [47] Liang, Xiao, et al. "Thermodynamics and evaporation of perfect fluid dark matter black hole in phantom background." *The European Physical Journal C* 83.11 (2023): 1009.
- [48] Abbas, G., and R. H. Ali. "Thermal fluctuations, quasi-normal modes and phase transition of the charged AdS black hole with perfect fluid dark matter." *The European Physical Journal C* 83.5 (2023): 1-18.
- [49] Das, Anish, Ashis Saha, and Sunandan Gangopadhyay. "Investigation of circular geodesics in a rotating charged black hole in the presence of perfect fluid dark matter." *Classical and Quantum Gravity* 38.6 (2021): 065015.
- [50] Yu, Qin, Qi Xu, and Jun Tao. "Thermodynamics and microstructures of Euler–Heisenberg black hole in a cavity." *Communications in Theoretical Physics* 75.9 (2023): 095402.
- [51] Ruffini, Remo, Yuan-Bin Wu, and She-Sheng Xue. "Einstein-Euler-Heisenberg theory and charged black holes." *Physical Review D* 88.8 (2013): 085004.
- [52] Magos, Daniela, and Nora Breton. "Thermodynamics of the Euler-Heisenberg-AdS black hole." *Physical Review D* 102.8 (2020): 084011.
- [53] Ye, Xu, et al. "QED effects on phase transition and Ruppeiner geometry of Euler-Heisenberg-AdS black holes." *Chinese Physics C* 46.11 (2022): 115102.
- [54] Ma, Shi-Jie, et al. "Euler-Heisenberg black hole surrounded by perfect fluid dark matter." arXiv preprint arXiv:2401.03187 (2024).

- [55] Bardeen, James. "Non-singular general relativistic gravitational collapse." Proceedings of the 5th International Conference on Gravitation and the Theory of Relativity. 1968.
- [56] Ayon-Beato, Eloy, and Alberto Garcia. "Regular black hole in general relativity coupled to nonlinear electrodynamics." *Physical review letters* 80.23 (1998): 5056.
- [57] Ayón-Beato, Eloy, and Alberto Garcia. "The Bardeen model as a nonlinear magnetic monopole." *Physics Letters B* 493.1-2 (2000): 149-152.
- [58] Gao, Changjun. "Black holes with many horizons in the theories of nonlinear electrodynamics." *Physical Review D* 104.6 (2021): 064038.
- [59] Claudel, Clarissa-Marie, Kumar Shwetketu Virbhadra, and George FR Ellis. "The geometry of photon surfaces." *Journal of Mathematical Physics* 42.2 (2001): 818-838.
- [60] Guo, Sen, et al. "The shadow and photon sphere of the charged black hole in Rastall gravity." *Classical and Quantum Gravity* 38.16 (2021): 165013.
- [61] Wei, Shao-Wen, et al. "Static spheres around spherically symmetric black hole spacetime." *Physical Review Research* 5.4 (2023): 043050.
- [62] Heydarzade, Yaghoub, and Vitalii Vertogradov. "Dynamical Photon Spheres in Charged Black Holes and Naked Singularities." *arXiv e-prints* (2023): arXiv-2311.
- [63] Franzin, Edgardo, Stefano Liberati, and Vania Vellucci. "From regular black holes to horizonless objects: quasi-normal modes, instabilities and spectroscopy." *Journal of Cosmology and Astroparticle Physics* 2024.01 (2024): 020.
- [64] Koga, Yasutaka, et al. "Dynamical photon sphere and time evolving shadow around black holes with temporal accretion." *Physical Review D* 105.10 (2022): 104040.
- [65] Grandclément, Philippe. "Light rings and light points of boson stars." *Physical Review D* 95.8 (2017):
- [66] Hod, Shahar. "On the number of light rings in curved spacetimes of ultra-compact objects." *Physics Letters B* 776 (2018): 1-4.
- [67] da Silva, Luís F. Dias, et al. "Photon rings as tests for alternative spherically symmetric geometries with thin accretion disks." *Physical Review D* 108.8 (2023): 084055.
- [68] Koga, Yasutaka, and Tomohiro Harada. "Stability of null orbits on photon spheres and photon surfaces." *Physical Review D* 100.6 (2019): 064040.

- [69] Cunha, Pedro VP, Carlos AR Herdeiro, and João PA Novo. "Light rings on stationary axisymmetric spacetimes: blind to the topology and able to coexist." *Physical Review D* 109.6 (2024): 064050.
- [70] Mosani, Karim, Dipanjan Dey, and Pankaj S. Joshi. "Globally visible singularity in an astrophysical setup." *Monthly Notices of the Royal Astronomical Society* 504.4 (2021): 4743-4750.
- [71] Virbhadra, Kumar Shwetketu, and George FR Ellis. "Schwarzschild black hole lensing." *Physical Review D* 62.8 (2000): 084003. Virbhadra, K. S. "Relativistic images of Schwarzschild black hole lensing." *Physical Review D* 79.8 (2009): 083004.
- [72] Sadeghi, Jafar, and Mohammad Ali S. Afshar. "The Role of Topological Photon Spheres in Constraining the Parameters of Black Holes." arXiv preprint arXiv:2405.06568 (2024).